Supplementary data

Different pretreatment methods combined with subsequent activation to convert waste eucalyptus bark into porous carbon electrode materials for supercapacitors

Kui Li [a, b], Zheng Liu *, [a, b], Xiangmeng Ma [a, b], Qingge Feng [a, b], Dongbo Wang [a, b], Dachao Ma [a, b]

[a] *School of Resources, Environment and Materials, Guangxi University, Nanning 530004, Guangxi, China.*

[b] *Key Laboratory of Environmental Protection (Guangxi University), Education Department of Guangxi Zhuang Autonomous Region, Guangxi Nanning 530004, China.*

** Corresponding author.*

E-mail addresses: zhengl99@gxu.edu.cn (Zheng Liu).

Electrochemical measurement methods

The electrochemical performance of electrode was firstly investigated in a three-electrode system using 6M KOH as the electrolyte. BPC, acetylene black and polytetrafluoroethylene binder were mixed together to give a weight ratio of 80:15:5 in ethanol, and formed slurry that was pressed onto a nickel foam current collector (1×1 cm^2) to afford working electrodes. The working electrodes were pressed under 10 MPa for 10 s and then dried under vacuum at 60 °C for 12 h for later tests, the mass loading of the active materials (including BPC, acetylene black and PTFE) in each working electrode determined as ~ 3.0 mg cm^{-2}. A platinum foil electrode (1 × 2 cm^2) and an Hg/HgO electrode were used as the counter electrode and reference electrode in a standard three-electrode setup, respectively. Cyclic voltammetry (CV), galvanostatic charge/discharge (GCD) and electrochemical impedance spectroscopy (EIS) in a frequency range of 100 kHz to 10 mHz at the open circuit potential with 5 mV amplitude were used to study the capacitive performance of the samples. In a three-electrode system, the specific capacitances were calculated from the charge-discharge curves according to the following equation:

$$C = \frac{I\Delta t}{m\Delta V} \qquad \text{(S1)}$$

Where C (F g^{-1}) is the specific capacitance; I (A) is the discharge current; Δt (s) is the discharge time; m (mg) is the mass of the active materials; ΔV (V) is the potential window.

The symmetric aqueous supercapacitors in 6 M KOH and 1 M Na_2SO_4 aqueous solution were assembled in a 2032 stainless steel coin cell using non-woven fabric to separate the two working electrodes with the same size and active material loadings of ~3.0 mg cm^{-2} on each working electrode. The symmetric solid-state supercapacitor was built face-to-face by using two same PBPC-600 electrodes, which were immersed into carboxymethylcellulose sodium/sodium sulfate (CMC-Na/Na_2SO_4) gel electrolyte with a non-woven fabric separator. The CMC-Na/Na_2SO_4 gel here was prepared as follows: 3 g CMC-Na powder (viscosity: 1200 mPa s) was dissolved into 50 mL 6 mol L^{-1} Na_2SO_4 solution under stirring at 70 °C until a transparent gel obtained. CV, GCD, EIS in a frequency range of 100 kHz to 10 mHz at the open circuit potential with 5 mV amplitude and 10000 charge-discharge cycles were studied to evaluate the performance of symmetric supercapacitors. For the symmetric supercapacitors, the specific capacitances, specific energy density and specific power density were calculated from the charge-discharge curves according to the following equation:

$$C = \frac{4I\Delta t}{m\Delta V} \qquad \text{(S2)}$$

$$E = \frac{1}{2} \times \frac{1}{4} \times C\Delta V^2 \qquad \text{(S3)}$$

$$P = \frac{3600E}{\Delta t} \qquad \text{(S4)}$$

Where C (F g^{-1}) is the specific capacitance; I (A) is the discharge current; Δt (s) is the discharge time; m (mg) is the mass of the active materials; ΔV (V) is the potential window. E (Wh kg^{-1}) is the average energy density; P (W kg^{-1}) is the average power density.

Figures and tables

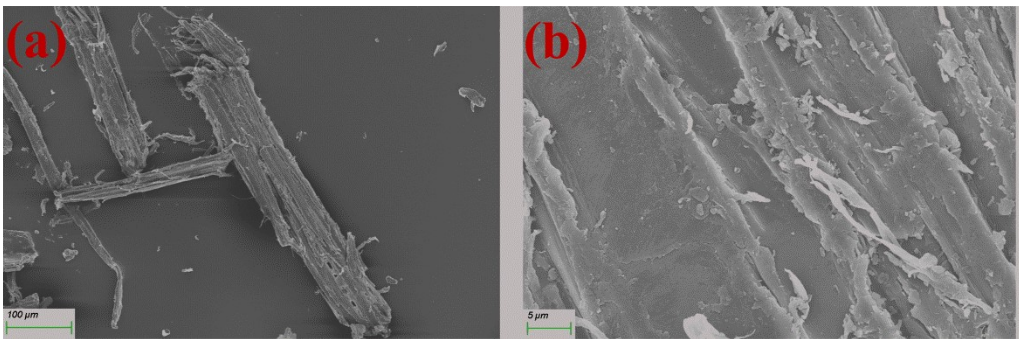

Fig. S1 SEM images of waste eucalyptus bark.

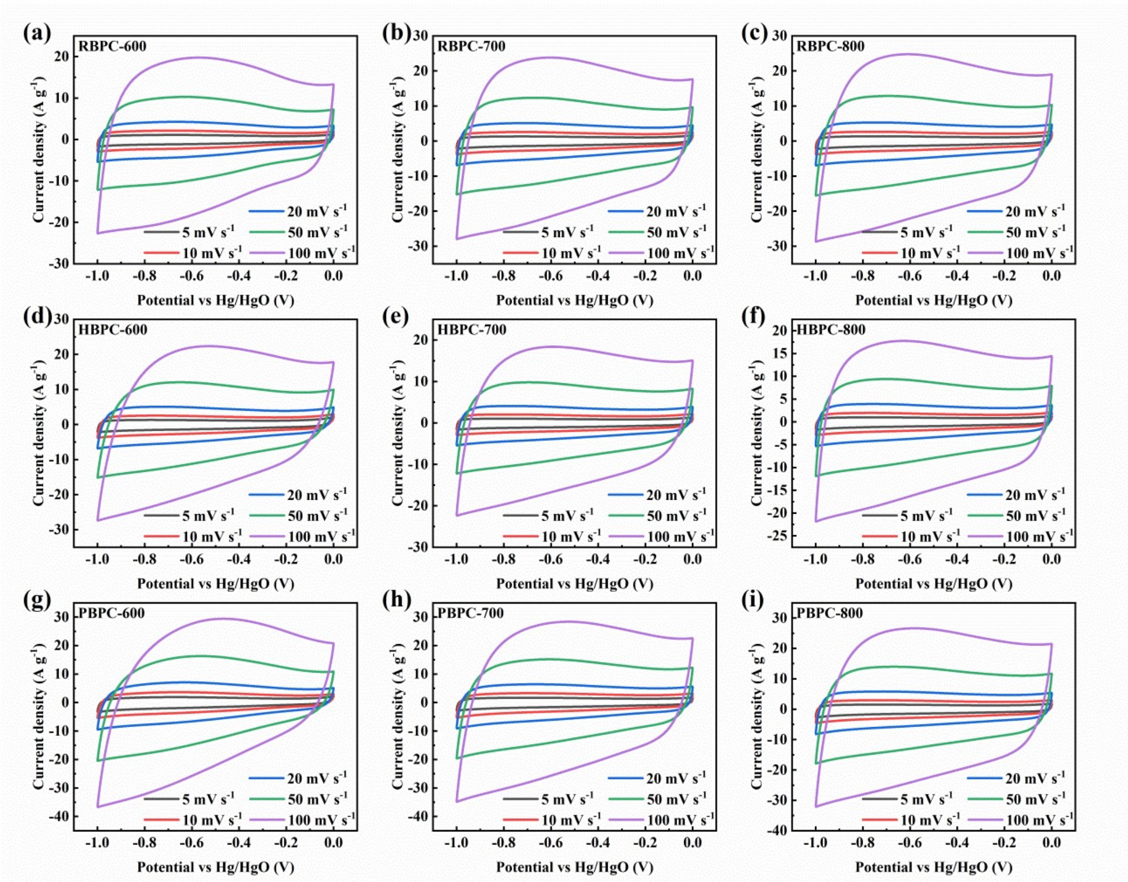

Fig. S2 CV curves of BPCs in a three-electrode system using 6 M KOH as the electrolyte.

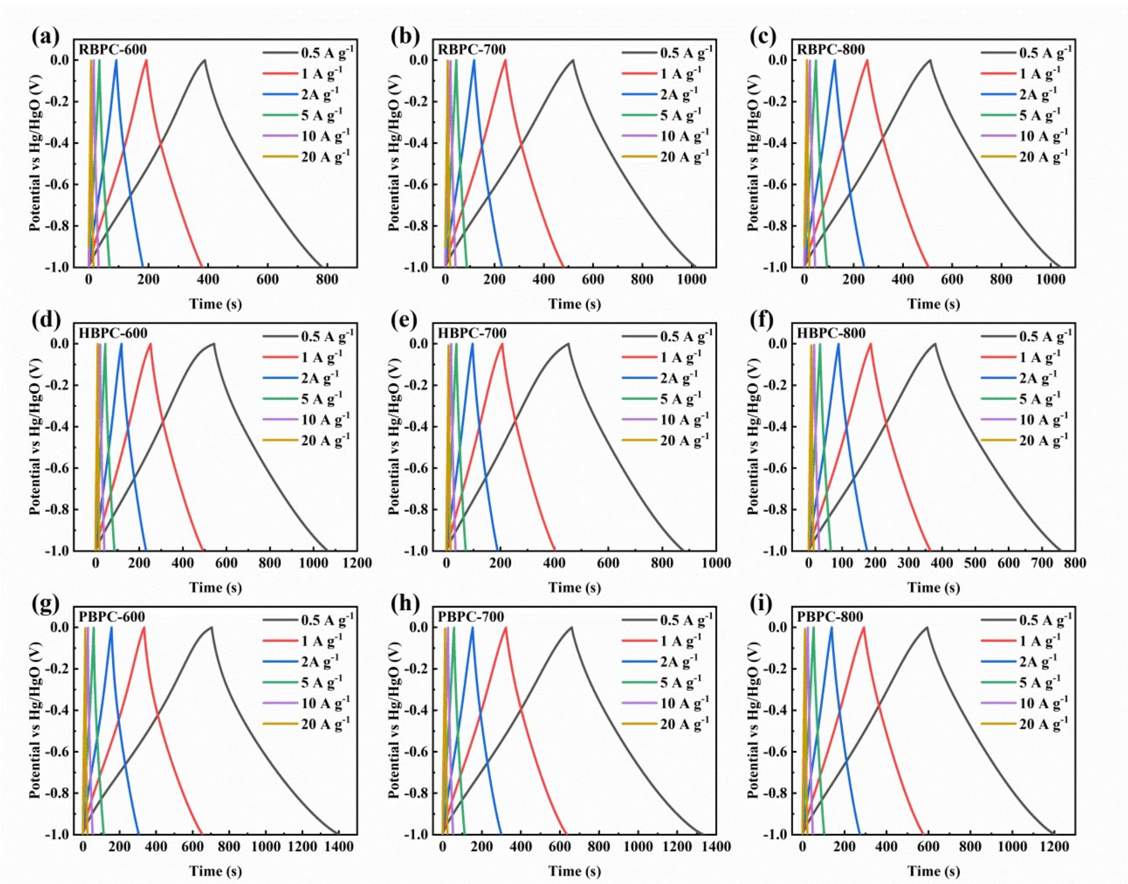

Fig. S3 GCD curves of BPCs in a three-electrode system using 6 M KOH as the electrolyte.

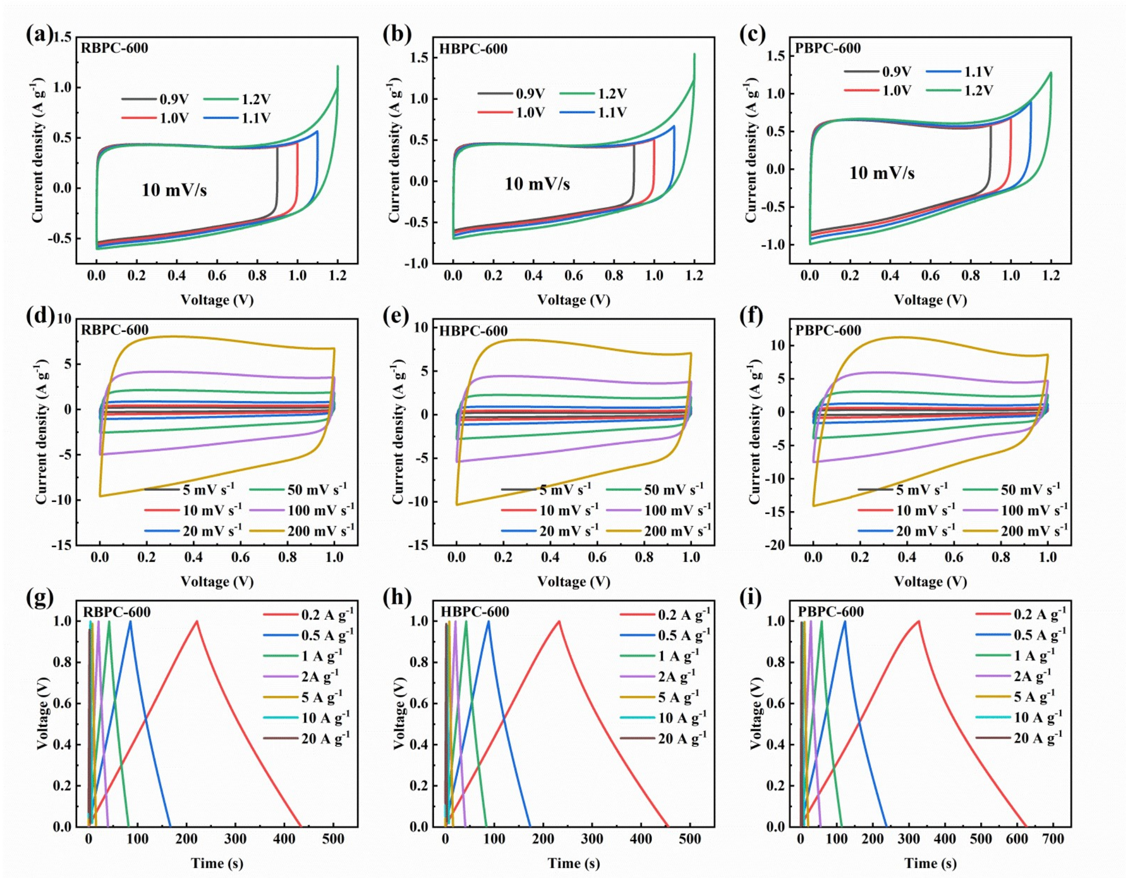

Fig. S4 Supercapacitance performance in a two-electrode system using 6M KOH as electrolyte: CV curves at a scan rate of 10 mV s^{-1} under different operating voltage of (a) RBPC-600, (b) HBPC-600 and (c) PBPC-600; CV curves at different scan rate of (d) RBPC-600, (e) HBPC-600 and (f) PBPC-600; GCD curves under different current density of (g) RBPC-600, (h) HBPC-600 and (i) PBPC-600.

Table S1 Comparison of the specific capacitance of PBPC-600 electrode with some reported carbon materials.

Materials	Electrolyte/ 3E	Specific capacitance (F g^{-1})	Reference
Hierarchical porous active carbon from fallen leaves	6M KOH	310.0 (0.5 A g^{-1})	1
Activated biomass carbon made from bamboo	3M KOH	293.0 (0.5 A g^{-1})	2
Tea-leaves based nitrogen-doped porous carbon	2M KOH	296.0 (0.5 A g^{-1})	3
graphene-like activated carbon derived from rice straw	3M KOH	255.0 (0.5 A g^{-1})	4
Rose-derived 3D carbon nanosheets	6M KOH	208.0 (0.5 A g^{-1})	5
Porous carbon derived from lotus seedpod shell	3M KOH	165.0 (0.5 A g^{-1})	6
Superhydrophilic carbon derived from sweet potato leaves	6M KOH	296.0 (0.5 A g^{-1})	7

Porous carbon derived from sorghum stalk	6M KOH	216.5 (0.5 A g^{-1})	8
Crosscutting bamboo-derived porous carbon	6M KOH	280.0 (0.5 A g^{-1})	9
Porous carbon derived from ginkgo leaves	6M KOH	323.2 (0.5 A g^{-1})	10
Biomass porous carbon derived from waste eucalyptus bark (PBPC-600)	6M KOH	349.4 (0.5 A g^{-1})	This work

Table S2 Comparison of the energy density of the PBPC-600 based symmetric quasi-solid-state supercapacitor with recently published carbon-based aqueous symmetric supercapacitors.

Electrode materials	Electrolyte	Max energy density (Wh kg^{-1})	Reference
Activated carbon synthesized from oil palm kernel shell	1 M Na_2SO_4	7.4 (300.0 W kg^{-1})	11
Porous carbon derived from sorghum stalk	0.5 M Na_2SO_4	9.8 (225.4 W kg^{-1})	8
Peanut shells-derived 3D porous carbon	PVA/Li_2SO_4	9.0 (380.0 W kg^{-1})	12
High graphitic biomass porous carbon	1 M Na_2SO_4	14.2 (218.8 W kg^{-1})	13
Monolithic carbon sponge	PVA/ KOH	5.6 (250.0 W kg^{-1})	14
Graphitic hierarchical porous carbon nanosheets	1 M Na_2SO_4	11.7 (80.0 W kg^{-1})	15
Honeycomb-like biomass carbon material	1 M Na_2SO_4	11.1 (20.0 W kg^{-1})	16
Tobacco-stem-derived porous carbon	1 M Na_2SO_4	7.8 (444.0 W kg^{-1})	17
O, N-doped porous carbon derived from bamboo shoots shells	1 M Na_2SO_4	13.2 (546.6 W kg^{-1})	18
Biomass porous carbon derived from waste eucalyptus bark (PBPC-600)	CMC-Na/Na_2SO_4 gel	15.0 (160.0 W kg^{-1})	This work

References

1 Y.-T. Li, Y.-T. Pi, L.-M. Lu, S.-H. Xu and T.-Z. Ren, *J. Power Sources*, 2015, **299**, 519-528.

2 G. Zhang, Y. Chen, Y. Chen and H. Guo, *Mater. Res. Bull.*, 2018, **102**, 391-398.

3 G. Ma, J. Li, K. Sun, H. Peng, E. Feng and Z. Lei, *J. Solid State Electr.*, 2016, **21**, 525-535.

4 K. M. Horax, S. Bao, M. Wang and Y. Li, *Chinese Chem. Lett.*, 2017, **28**, 2290-2294.

5 C. Zhao, Y. Huang, C. Zhao, X. Shao and Z. Zhu, *Electroch. Acta*, 2018, **291**, 287-296.

6 J. Pu, W. Kong, C. Lu and Z. Wang, *Ionics*, 2014, **21**, 809-816.

7 R. Fu, C. Yu, S. Li, J. Yu, Z. Wang, W. Guo, Y. Xie, L. Yang, K. Liu, W. Ren and J. Qiu, *Green Chem.*, 2021, **23**, 3400-3409.

8 G. Ma, F. Hua, K. Sun, Z. Zhang, E. Feng, H. Peng and Z. Lei, *RSC Adv*, 2016, **6**, 103508-103516.

9 J. Han, Y. Ping, S. Yang, Y. Zhang, L. Qian, J. Li, L. Liu, B. Xiong, P. Fang and C. He, *Diam. Relat. Mater.*, 2020, **109**, 108044.

10 Y. Wang, C. Shao, S. Qiu, Y. Zhu, M. Qin, Y. Meng, Y. Wang, H. Chu, Y. Zou, C. Xiang, J.-L. Zeng, Z. Cao, F. Xu and L. Sun, *Diam. Relat. Mater.*, 2019, **98**, 107475.

11 I. I. Misnon, N. K. M. Zain and R. Jose, *Waste Biomass Valori.*, 2018, **10**, 1731-1740.

12 P. A. Le, V. Q. Le, N. T. Nguyen and T. V. B. Phung, *Appl. Nanosci.*, 2022.

13 Y. Tan, Z. Xu, L. He and H. Li, *J. Energy Storage*, 2022, **52**, 104889.
14 X. Jing, L. Wang, K. Qu, R. Li, W. Kang, H. Li and S. Xiong, *ACS Appl. Energ. Mater.*, 2021, **4**, 6768-6776.
15 P. Li, H. Xie, Y. Liu, J. Wang, Y. Xie, W. Hu, T. Xie, Y. Wang and Y. Zhang, *J. Power Sources*, 2019, **439**, 227096.
16 K. Zhao, L. Zhao, W. Zhou, L. Rao, S. Wen, Y. Xiao, B. Cheng and S. Lei, *J. Energy Storage*, 2022, **52**, 104910.
17 H. Wang, L. Yang, G. Liu and M. Li, *ChemistrySelect*, 2021, **6**, 532-537.
18 J. Han, Q. Li, J. Wang, J. Ye, G. Fu, L. Zhai and Y. Zhu, *J. Mater. Sci.: Mater. El.*, 2018, **29**, 20991-21001.